Inorg. Chem. **2002**, *41*, 4468–4477

Synthesis and Catalytic Application of Octahedral Lewis Base Adducts of Dichloro and Dialkyl Dioxotungsten(VI)

Fritz E. Kühn,*[,†] Wen-Mei Xue,[†] Ahmad Al-Ajlouni,[†,‡] Ana M. Santos,[†,§] Shuliang Zang,[†,⊥] Carlos C. Romão,[§] Georg Eickerling,[†] and Eberhardt Herdtweck[†]

Anorganisch-Chemisches Institut, Technischen Universität München, Lichtenbergstrasse 4, D-85747 Garching bei München, Germany, Department of Applied Chemical Science, Jordan University of Science and Technology, 22110 Irbid, Jordan, Instituto de Tecnologia Química e Biológica, Universidade Nova de Lisboa, Quinta do Marquês, EAN, Apt 127, 2781-901 Oeiras, Portugal, and Department of Chemistry, Liaoning University, 110036 Shenyang, Peoples Republic of China

Received January 2, 2002

Complexes of the composition $W(O)_2(Cl)_2L_2$ and $W(O)_2(R)_2L_2$ (R = Me, Et; L_2 = bidentate Lewis base ligand) have been prepared and are fully characterized (including an exemplary X-ray crystal structure of $W(O)_2(Cl)_2$(4,4′-di-*tert*-butyl-2,2′-bipyridine)). This latter compound crystallizes in the orthorhombic space group $P2_12_12_1$ with a = 8.3198(1) Å, b = 13.3224(2) Å, c = 18.0415(2) Å, and Z = 4. The title complexes are applied as catalysts in olefin epoxidation catalysis with *tert*-butyl hydroperoxide (TBHP) as the oxidizing agent. The W(VI) complexes display only moderate turnover frequencies but can be reused several times without loss of catalytic activity. The highest activity can be achieved at reaction temperatures of ca. 90 °C. Chloro derivatives are somewhat more active than alkyl complexes, and sterically less crowded complexes show also higher activities than their congeners with bulky ligands L_2. Kinetic examinations show that the catalyst formation is the rate determining step and it is observed that *tert*-butyl alcohol, the byproduct of the epoxidation reaction, acts as a competitor for TBHP, thus lowering the reaction velocity during the course of the reaction but not irreversibly destroying the catalyst.

Introduction

Transition metal oxo complexes have found applications as catalysts in industry scale epoxidation reactions and other oxo transfer processes for several decades.[1] Especially Mo(VI) oxo complexes have been under investigation, both to elucidate the catalytic mechanism and to broaden and optimize their field of applications.[2−11] In the past decade several new or improved Mo(VI) catalysts based on $Mo(O_2)_2OL_2$, $Mo(O)_2L_4$, and $Mo(O)_2(X)_2L_2$ emerged[5−11] and additionally other transition metal complexes also gained significant interest as oxidation catalysts, probably the most famous among them being the very versatile methyltrioxorhenium(VII) and its derivatives.[12,13] Despite all these new findings, the tungsten complexes of the composition $W(O)_2L_4$,

* Author to whom correspondence should be addressed. E-mail: fritz.kuehn@ch.tum.de.
† Technischen Universität München.
‡ Jordan University of Science and Technology.
§ Universidade Nova de Lisboa.
⊥ Liaoning University.

(1) (a) Sheldon, R. A. In *Applied Homogeneous Catalysis with Organometallic Compounds*; Cornils, B., Herrmann, W. A., Eds.; VCH: Weinheim, New York, 1996; Vol. 1. (b) Arzoumanian, H. *Coord. Chem. Rev.* **1998**, *180*, 191. (c) Holm, R. H. *Chem. Rev.* **1987**, *87*, 1401. (d) Holm, R. H. *Coord. Chem. Rev.* **1990**, *100*, 183. (e) Sheldon, R. A. *Recl. Trav. Chim. Pay. B* **1973**, *92*, 253. (f) Sheldon, R. A. *Recl. Trav. Chim. Pay. B* **1973**, *92*, 367. (g) Sheldon, R. A.; van Doorn, J. A. *J. Catal*. **1973**, *31*, 427. (h) Sheldon, R. A.; van Doorn, J. A. *J. Organomet. Chem*. **1975**, *94*, 115. (i) Chong, A. O.; Sharpless, K. B. *J. Org. Chem*. **1977**, *42*, 1587. (j) Mimoun, H. *J. Mol. Catal*. **1980**, *7*, 1. (k) Mimoun, H. *Angew. Chem., Int. Ed. Engl*. **1982**, *2*, 734.
(2) Chaumette, P.; Mimoun, M.; Saussine, L. *J. Organomet. Chem*. **1983**, *250*, 291.
(3) Roberts, S. A.; Young, C. G.; Kipke, C. A.; Cleland, W. E.; Yamanouchi, K.; Carducci, M. D.; Enemark, J. H. *Inorg. Chem*. **1990**, *29*, 3650.
(4) Trost, M. K.; Bergman, R. G. *Organometallics* **1991**, *10*, 1172.
(5) Belgacem, J.; Kress, J.; Osborn, J. A. *J. Chem. Soc., Chem. Commun*. **1993**, 1125.
(6) Teruel, H.; Sierralta, A. *J. Mol. Catal. A: Chemical* **1996**, *107*, 379.
(7) Glorius, F.; Pfaltz, A. *Org. Lett*. **1999**, *1*, 141.
(8) (a) Deubel, D. V.; Sundermeyer, J.; Frenking, G. *J. Am. Chem. Soc*. **2000**, *122*, 10101. (b) Wahl, G.; Kleinhenz, D.; Schorm, A.; Sundermeyer, J.; Stowasser, R.; Rummey, C.; Bringmann, G.; Fickert, C.; Kiefer, W. *Chem. Eur. J*. **1999**, *5*, 3237.
(9) (a) Gisdakis, P.; Yudanov, I. V.; Rösch, N. *Inorg. Chem*. **2001**, *40*, 3755. (b) Hroch, A.; Gemmecker, G.; Thiel, W. R. *Eur. J. Inorg. Chem*. **2000**, *1107* and references therein.
(10) Mitchell, J. M.; Finney, N. *J. Am. Chem. Soc.* **2001**, *123*, 862.

10.1021/ic0200085 CCC: $22.00
Published on Web 07/23/2002

$W(O)_2(Cl)_2L_2$, and $W(O)_2(R)_2L_2$ were not investigated in great detail with respect to applications in homogeneous oxidation catalysis with *t*-BuOOH (TBHP) as the oxidizing agent.[14] On the other hand, heterogeneous W(VI) compounds, W oxo cluster complexes, and WO_4^{2-} derivatives gained significant interest in oxidation catalysis, mainly with H_2O_2 as the oxidizing agent.[15] It is assumed that the epoxidation reactions with H_2O_2 proceed via peroxo tungsten complexes.[16]

Following our recent work on olefin epoxidation with TBHP catalyzed by complexes of the type $Mo(O)_2(X)_2L_2$ (X = Cl, Br) and $Mo(O)_2(R)_2L_2$ (R = Me, Et),[17−21] we decided to extend our examinations to the homologous W(VI) derivatives to compare their reactivity, applicability, and epoxidation mechanism to the above-mentioned Mo(VI) compounds. W(VI) complexes of the composition $W(O)_2(Cl)_2L_2$ were reported for the first time by Brisdon in 1967[22] and complexes of the composition $W(O)_2(R)_2L_2$ (R = alkyl) were reported by Schrauzer et al. in 1990.[23] However, in several cases the literature procedures toward the $W(O)_2(Cl)_2L_2$ complexes proved to be either complicated or having low yields so that improved synthetic strategies were necessary.[24,25] The variety of ligands L used was also quite small (usually the bidentate ligands 2,2′-bipyridine, 2,2′-phenanthroline, or solvent molecules, e.g. dimethoxyethane (DME)) prompting our use of some additional bidentate ligands L_2, which usually lead to more soluble complexes. In the present work we describe the preparation of a series of new $W(O)_2(R)_2L_2$ and $W(O)_2(X)_2L_2$ complexes and characterize their catalytic activity and kinetics in cyclooctene epoxidation.

Results and Discussion

Synthesis and Spectroscopic Studies. Dichlorodioxotungsten(VI) (**1**) derivatives were prepared by a similar synthetic strategy published previously for $W(O)_2(Cl)_2$(2,2′-bipyridine) (eq 1a).[22] In contrast to the poor solubility of

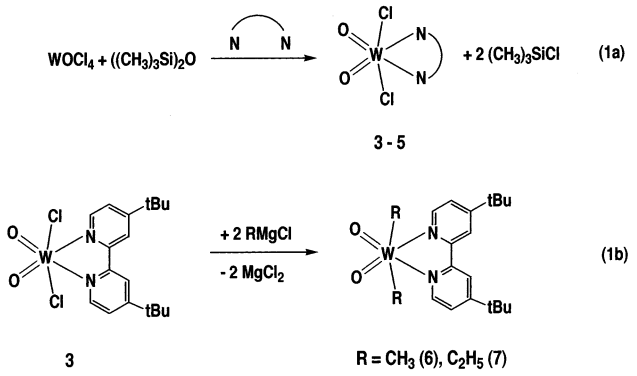

$W(O)_2(Cl)_2$(2,2′-bipyridine), compounds **2** and **3** are highly soluble in CH_2Cl_2, $CHCl_3$, THF, and other organic solvents. Compounds **4** and **5** are nearly insoluble in common organic solvents except in dimethyl formamide (DMF). However,

(11) Valente, A. A.; Gonçalves, I. S.; Lopes, A. D.; Rodríguez-Borges, J. E.; Pillinger, M.; Romão, C. C.; Rocha, J.; García-Mera, X. *New J. Chem.* **2001**, *25*, 959.

(12) (a) Owens, G. S.; Arias, J.; Abu-Omar, M. M. *Catal. Today* **2000**, *55*, 317. (b) Adam, W.; Mitchell, C. M.; Saha-Möller, C. R.; Weichold, O. (Hrsg.: B. Meunier) *Struct Bonding* **2000**, *97*, 237. (c) Kühn, F. E.; Herrmann, W. A. (Hrsg.: B. Meunier) *Struct Bonding* **2000**, *97*, 211. (d) Espenson, J. H.; Abu-Omar, M. M. *A.C.S. Adv. Chem.* **1997**, *253*, 3507.

(13) (a) Romão, C. C.; Kühn, F. E.; Herrmann, W. A. *Chem. Rev.* **1997**, *97*, 3197. (b) Herrmann, W. A.; Kühn, F. E. *Acc. Chem. Res.* **1997**, *30*, 169.

(14) (a) Wong, Y. L.; Yang, Q. C.; Zhou, Z. Y.; Lee, H. K.; Mak, T. C. W.; Ng, D. K. P. *New J. Chem.* **2001**, *25*, 353. (b) Herrmann, W. A.; Haider, J. J.; Fridgen, J.; Lobmaier, G. M.; Spiegler, M. *J. Organomet. Chem.* **2000**, *603*, 69. (c) Herrmann, W. A.; Fridgen, J.; Lobmaier, G. M.; Spiegler, M. *New J. Chem.* **1999**, *23*, 5. (d) Wong, Y. L.; Ma, J. F.; Lwa, W. F.; Yan, Y.; Wong, W. T.; Thang, Z. Y.; Mak, T. C. W.; Ng, D. K. P. *Eur. J. Inorg. Chem.* **1999**, 313. (e) Wong, Y. L.; Yan, Y.; Chan, E. S. H.; Mak, T. C. W.; Ng, D. K. P. *J. Chem. Soc.; Dalton Trans.* **1998**, 3057. (f) Adam, W.; Putterlik, J.; Schuhmann, R.; Sundermeyer, J. *Organometallics* **1996**, *15*, 4586. (g) Arzoumanian, H.; Kerentzien, H.; Teruel, H. *J. Chem. Soc., Chem. Commun.* **1991**, 55.

(15) (a) De Vos, D. E.; Sels, B. F.; Jacobs, P. A. *Adv. Catal.* **2002**, *46*, 1. (b) Weinstock, I. A.; Barbuzzi, E. M. G.; Wemple, M. W.; Cowan, J. J.; Reiner, R. S.; Sonnen, D. M.; Heintz, R. A.; Bond, J. S.; Hill, C. L. *Nature* **2001**, *414*, 191. (c) Ichihara, J. *Tetrahedron Lett.* **2001**, *42*, 695. (d) Deubel, D. V. *J. Phys. Chem. A* **2001**, *105*, 4765. (e) Hoegaerts, D.; Sels, B. F.; de Vos, D. E.; Verpoort, F.; Jacobs, P. A. *Catal. Today* **2000**, *60*, 209. (f) Vassilev, K.; Stamenova, R.; Tsvetanov, C. *React. Funct. Polym.* **2000**, *46*, 165. (g) Kozhernikov, I. V. *Chem. Rev.* **1998**, *98*, 171. (h) Sato, K.; Aoki, M.; Ogawa, M.; Hashimoto, T.; Panyella, D.; Noyori, R. *Bull. Chem. Soc. Jpn.* **1997**, *70*, 905. (i) Gelbard, G.; Raison, F.; Roditi-Lachter, E.; Thouvenot, R.; Ouahab, L.; Grandjean, D. *J. Mol. Catal. A: Chemical* **1996**, *114*, 77. (j) Duncan, D. C.; Chambers, R. C.; Hecht, E.; Hill, C. L. *J. Am. Chem. Soc.* **1995**, *117*, 681. (k) Griffith, W. P.; Slawin, A. M. Z.; Thompson, K. M.; Williams, D. J. *J. Chem. Soc., Chem. Commun.* **1994**, 569. (l) Ballistreri, F. P.; Tomaselli, G. A.; Toscano, R. M.; Conte, V.; Di Furia, F. *J. Mol. Catal.* **1994**, *89*, 295. (m) Dickman, M. H.; Pope M. T. *Chem. Rev.* **1994**, *94*, 569. (n) Dengel, A. C.; Griffith, W. P.; Parkin, B. C. *J. Chem. Soc., Dalton Trans.* **1993**, 2683. (o) C. Venturello, C.; Alneri, E.; Ricci, M. *J. Org. Chem.* **1983**, *48*, 3831. (p) Payne, G. B.; Williams, P. H. *J. Org. Chem.* **1959**, *24*, 54.

(16) (a) Salles, C.; Aubry, R.; Thouvenot, F.; Robert, C.; Dorémieux-Morin, C.; Chottard, H.; Ledon, H.; Jeannin, Y.; Brégeault, J. M. *Inorg. Chem.* **1994**, *33*, 871. (b) Neumann, R.; Khenkin, A. M. *J. Org. Chem.* **1994**, *59*, 7577. (c) Aubry, C.; Chottard, G.; Platzer, N.; Brégeault, J. M.; Thouvenot, R.; Chauveau, F.; Huet, C.; Ledon, H. *Inorg. Chem.* **1991**, *30*, 4409.

(17) Santos, A. M.; Kühn, F. E.; Bruus-Jensen, K.; Lucas, I.; Romão, C. C.; Herdtweck, E. *J. Chem. Soc., Dalton Trans.* **2001**, 1332.

(18) Kühn, F. E.; Santos, A. M.; Gonçalves, I. S.; Romão, C. C.; Lopes, A. D. *Appl. Organomet. Chem.* **2001**, *15*, 43.

(19) (a) Kühn, F. E.; Santos, A. M.; Lopes, A. D.; Gonçalves, I. S.; Herdtweck, E.; Romão, C. C. *J. Mol. Catal. A: Chemical* **2000**, *164*, 25. (b) Groarke, M.; Gonçalves, I. S.; Herrmann, W. A.; Kühn, F. E. *J. Organomet. Chem.* **2002**, *649*, 108.

(20) Kühn, F. E.; Lopes, A. D.; Santos, A. M.; Herdtweck, E.; Haider, J. J.; Romão, C. C.; Gil Santos, A. *J. Mol. Catal., A: Chemical* **2000**, *151*, 147.

(21) Kühn, F. E.; Herdtweck, E.; Haider, J. J.; Herrmann, W. A.; Gonçalves, I. S.; Lopes, A. D.; Romão, C. C. *J. Organomet. Chem.* **1999**, *583*, 3.

(22) Brisdon, B. J. *Inorg. Chem.* **1967**, *6*, 1791.

(23) Zhang, C.; Schlemper, E. O.; Schrauzer, G. N. *Organometallics* **1990**, *9*, 1016.

(24) (a) Dreisch, K.; Anderson C.; Stålhandske, C. *Polyhedron* **1993**, *12*, 303. (b) Dreisch, K.; Anderson C.; Stålhandske, C. *Polyhedron* **1992**, *11*, 2143. (c) Herrmann, W. A.; Thiel, W. R.; Herdtweck, E. *Chem. Ber.* **1990**, *123*, 271. (d) Gibson, V. G.; Kee, T. P.; Shaw, A. *Polyhedron* **1988**, *7*, 579. (e) Wet, J. F. D.; Caira, M. R.; Gellatly, B. J. *Acta Crystallogr. B* **1978**, 762. (f) Khodadad, P.; Viossat, B. *J. Less Common Met.* **1976**, *46*, 25. (g) Florian, L. R.; Corey, E. R. *Inorg. Chem.* **1968**, *7*, 722. (h) Hull, C. G.; Stiddard, M. H. B. J. *Chem. Soc., Inorg. Phys. Theor.* **1966**, 1633.

(25) (a) Wong, Y. L.; Ma, J. F.; Xue, F. *Organometallics* **1999**, *18*, 5075. (b) Boncella, J. M.; Wang, S. Y. S.; van der Lende, D. D. *J. Organomet. Chem.* **1997**, *530*, 59. (c) Onishi, M.; Ikimoto, K.; Hiraki, K. *Bull. Chem. Soc. Jpn.* **1993**, *66*, 1849. (d) Eagle, A. A.; Young, C. G.; Tiekink, E. R. T. *Organometallics* **1992**, *11*, 2934. (e) Eagle, A. A.; Tiekink, E. R. T.; Young, C. G. *J. Chem. Soc., Chem. Commun.* **1991**, 1746.

Chart 1

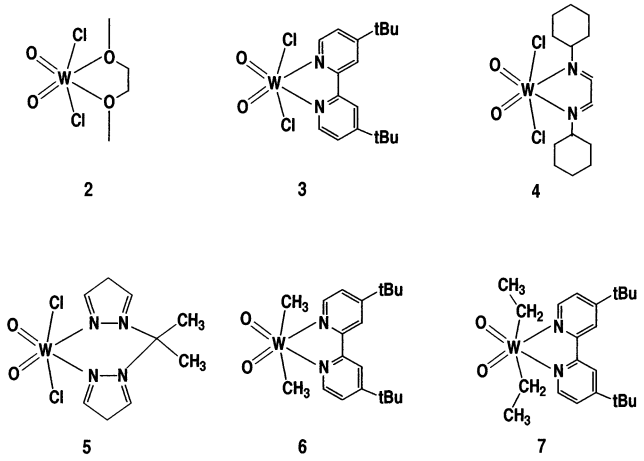

DMF dissociates the ligand BPP (2,2-bis(1-pyrazolyl)-propane) from the metal center and only ^{1}H NMR signals of the free ligand are detected. Compounds **6** and **7** were synthesized by starting from the chloro derivative $W(O)_2(Cl)_2$(*t*-bubipy) (eq 1b). This is different from the literature method for the preparation of $W(O)_2(R)_2$(2,2′-bipyridine), where the bromo derivative was used as starting material. The chloro derivative has the advantage of being very easily prepared. The bromo derivative is much less convenient to prepare and therefore is a far less desirable starting material. Compounds **6** and **7** are soluble in all common organic solvents. All complexes examined here are air-stable. The formulas of compounds **2**−**7** are given in Chart 1.

The IR spectra of the compounds exhibit two strong ν(W═O) vibrations at 942−960 and 897−920 cm^{-1} for the characteristic asymmetric and symmetric stretching of the *cis*-$[WO_2]^{2+}$ moiety. The ν(W═O) vibrations of $W(O)_2(Cl)_2$(2,2′-bipyridine) have been reported to show up at 954 and 913 cm^{-1}.[22,26a]

The ^{1}H NMR chemical shifts of the metal attached alkyl groups of complexes **6** and **7** are very similar to that of the closely related but significantly less soluble complexes described by Schrauzer et al.[23] It has to be noted that the chemical shifts of the alkyl groups are temperature and solvent dependent, shifting up to ca. 0.5 ppm (see also kinetics section below).

Two of the compounds, namely the derivatives **3** and **7**, as well as the ligand 4,4′-di-*tert*-butyl-2,2′-bipyridine (*t*-bubipy) and compound **1**,[26b] have been exemplary examined by thermogravimetry (TG). The ligand sublimes completely, starting at 150 °C. Complex **1** displays the onset of its decomposition at 291 °C. The observed mass loss is equivalent to the loss of two Cl ligands. The Cl-derivative **3** displays the first decomposition onset at 169 °C. The decomposition takes place in two clearly distinct steps, where the first step is again divided in two "substeps" which are not clearly distinct from one another. The two parts are approximately equal in mass loss and sum up to ca. 46% of the original mass. A loss of the *t*-bubipy ligand would account for 48.35%, so that we assume the first distinct decomposition step is due to the loss of the *t*-bubipy ligand, which breaks apart during the decomposition. The second decomposition step has its onset at 293 °C, being nearly identical with the decomposition onset of compound **1**. This gives additional evidence that the remaining residue at this temperature consists mainly of $W(O)_2(Cl)_2$. The ethyl derivative **7** decomposes with only one pronounced step, the onset being located at 224 °C. The mass loss is equal to ca. 56% of the original mass. Clear substeps cannot be detected. The ethyl moieties and the *t*-bubipy ligand together account for 60.0% of the complex mass. It is therefore likely to assume that these ligands are lost, leaving only small amounts of C, H, and N in the remaining residue. This is in accord with the elementary analysis of the residues of both complexes **3** and **7** which contain only traces of C, H, N, and Cl (in the case of complex **3**) and consist mainly of W and O. Both complexes **3** and **7** start decomposing at significantly higher temperatures than the sublimation temperature of *t*-bubipy. This fact demonstrates the strength of the N−W interaction in these complexes.

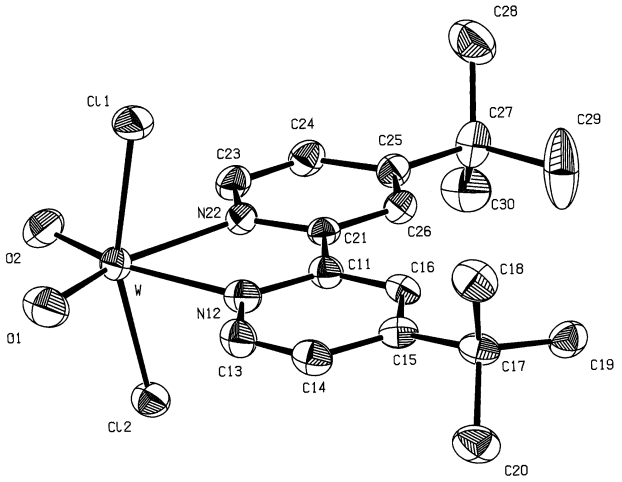

Figure 1. PLATON representation of compound **3**. The thermal ellipsoids are given at a 50% probability level.

X-ray Crystallography. The molecular structure of compound **3** (Figure 1) was determined by single-crystal X-ray crystallography. The experimental details are given in Table 1; key bond distances and angles are listed in Table 2. The tungsten atom is coordinated as a distorted octahedron in which the two chloride atoms are trans and the two oxygen atoms cis to each other. The bond distances for W−Cl, W═O, and W−N are well within the range found for related compounds.[27] As would be expected, the W−F bond distance in the previously reported complex $W(O)_2(F)_2$(2,2′-bipyridine) is approximately 0.4 Å shorter than the W−Cl bond. Bond distances and angles in the *t*-bubipy ligand are unexceptional and do not require further comment.

(26) (a) Soptrajanov, B.; Trpkovska, M.; Pejov, L. *Croat. Chem. Acta* **1999**, *72*, 663. (b) Eliseev, S. S.; Malysheva, L. E. *Zh. Neorg. Khim*. **1976**, *21*, 1397.

(27) (a) Allen, F. H.; Kennard, O. 3D Search and Research Using the Cambridge Structural Database. In *Chemical Design Automation News* **1993**, *8*, 1, 31−37. (b) 233218 entries CCDC refcode VESJAE; TOFLEF; KEMCUA; JEKZUU; JEKZOO.

Table 1. Crystallographic Data for $W(O)_2(Cl)_2$(4,4′-di-*tert*-butyl-2,2′-bipyridine) (**3**)

chemical formula	$C_{18}H_{24}Cl_2N_2O_2W$
fw, g mol $^{-1}$	555.13
cryst syst	orthorhombic
space group	$P2_12_12_1$ (no. 19)
a, Å	8.3198(1)
b, Å	13.3224(2)
c, Å	18.0415(2)
V, Å^3	1999.71(4)
Z	4
T, K	173
ρ_{calcd}, g cm^{-3}	1.844
λ(Mo Kα), Å	0.71073
μ, mm^{-1}	6.057
R1[a]	0.0265
wR2[b]	0.0600

[a] $R1 = \sum(||F_o| - |F_c||)/\sum|F_o|$. [b] $wR2 = [\sum w(F_o^2 - F_c^2)^2/\sum w(F_o^2)^2]^{1/2}$.

Table 2. Selected Bond Lengths (Å) and Angles (deg) for Compound **3**

W−O(1)	1.720(6)	Cl(1)−W−Cl(2)	160.92(5)
W−O(2)	1.745(5)	O(1)−W−O(2)	104.5(3)
W−Cl(1)	2.3442(15)	O(1)−W−N(12)	93.0(2)
W−Cl(2)	2.3542(15)	O(1)−W−N(22)	162.2(2)
W−N(12)	2.278(7)	O(2)−W−N(12)	162.4(2)
W−N(22)	2.278(6)	O(2)−W−N(22)	93.3(2)
		N(12)−W−N(22)	69.2(2)

Dioxotungsten(VI) Complexes in Olefin Epoxidation Catalysis: Activity and Selectivity. Complexes of the composition $Mo(O)_2(X)_2L_2$[17−21] have been examined as catalyst precursors in epoxidation catalysis with TBHP as oxidizing agent and have proven to give rise to moderately active to very active catalyst systems. The nature of the active species, however, has been examined in detail only very recently.[28] To gain insight into the catalytic behavior of the related W(VI) derivatives presented in this work, they were examined under similar reaction conditions. Since we assumed that the W(VI) complexes would be less active but more stable catalysts than their Mo congeners we hoped to get a closer insight into the kinetics of the catalytic reaction and the true nature of the active species to compare these findings with the results obtained in the Mo case[28] and obtain a more complete picture of the catalytic cycles. Table 3 summarizes the catalytic performance of the complexes examined. Blank reactions have been performed and, as expected, without catalyst no significant epoxide formation was observed under the applied conditions. In general, the reaction velocity is relatively low, especially at temperatures below 70 °C (see below for more details). However, the epoxide yield keeps increasing until reaching the maximum of ca. 100% in all cases, demonstrating the pronounced stability of the catalysts under the reaction conditions. All catalytic reactions show, in general, the same time-dependent curve as the related Mo(VI) species.[17−21] The formation of products other than the desired epoxides is not observed to a significant extent.

Table 3. Turnover Frequencies and Yield of Cyclooctene Epoxide in the Presence of Dioxotungsten(VI) Derivatives as Catalysts[a]

catalyst	temp (°C)	TOF (mol/mol cat.·h)	yield of cyclooctene epoxide (%) 6 h	24 h
$W(O)_2(Cl)_2$ (**1**)	55	16	10	30
	70	21	34	∼100
	90	28	91	∼100
		10		
$W(O)_2(Cl)_2$(DME) (**2**)	55	10	10	27
	70	20	36	∼100
	90	23	75	∼100
$W(O)_2(Cl)_2$(*t*-bubipy) (**3**)	70	9	19	56
	90	18	34	63
$W(O)_2(Cl)_2$(CYDAB) (**4**)	55	4	4	7
	70	12	13	84
	90	26	42	∼100
$W(O)_2(Cl)_2$(BPP) (**5**)	70	20	12	67
$W(O)_2(Me)_2$(*t*-bubipy) (**6**)	90	15	30	∼100
$W(O)_2(Et)_2$(*t*-bubipy) (**7**)	90	12	28	∼100

[a] See text and the Experimental Section for reaction details. TOF were calculated after 10 min reaction time.

In the case of the $Mo(O)_2(X)_2L_2$ complexes the turnover frequency (TOF) is usually at least 1 order of magnitude higher than in the case of their tungsten homologues. For the chloro derivatives the TOFs for the Mo(VI) complexes range up to ca. 600 mol/(mol·h) and for the alkyl derivatives up to 150 mol/(mol·h) at 55 °C reaction temperature, if a catalyst:TBHP:substrate ratio of 0.1:200:100 is applied.[17−21]

The temperature effect on the epoxide yield was examined by GC methods with the complexes **1**, **2**, and **4** as examples, and the results are summarized in Table 3. Complex **1** was chosen because of its low sterical hindrance for the sake of comparison, complex **2** because it bears a weakly coordinating O-donor ligand with little sterical demand, and complex **4** because of its bulky N-donor ligand. It has to be noted, however, that in the case of compound **1** very likely a different reaction mechanism will occur than in the case of the octahedral Lewis base adducts **2** and **4** and their previously examined Mo congeners. Below 30 °C the reaction is extremely slow in all cases. At 55 °C, the reaction velocity is still very low in all cases, and the epoxide yields are below 30% after 24 h. More elevated temperatures accelerate the reaction significantly. At 90 °C, the maximum epoxide yield of ca. 100% is reached for all examined catalysts (with the exception of compound **3**) within 24 h. It has to be stated that all three complexes are soluble under the conditions applied. Due to the low concentrations and especially at elevated temperatures the complexes dissolve immediately. We therefore think that clearly other reasons than solubility problems are responsible for the observed activity differences (see below: kinetic examinations and ligand influence). The W(VI)-dioxo derivatives under investigation show higher thermal stability both in solution and in the solid state than the Mo(VI)-dioxo analogues[17−21] (see also TG results above for the solid state). In the case of some Mo(VI) derivatives, a temperature increase from 70 °C to 90 °C did not lead to a significant increase of the epoxide yield and in some cases even a yield reduction

(28) Kühn, F. E.; Groarke, M.; Bencze, É.; Herdtweck, E.; Prazeres, E.; Santos, A. M.; Calhorda, M. J.; Romão, C. C.; Gonçalves, I. S.; Lopes, A. D.; Pillinger, M. *Chem. Eur. J.* **2002**, 8, 2370.
(29) Pestovsky, O.; van Eldik, R.; Huston, P.; Espenson, J. H. *J. Chem. Soc., Dalton Trans.* **1995**, 133.
(30) Kühn, F. E.; Herrmann, W. A. *Chemtracts−Org. Chem.* **2001**, *14*, 59.

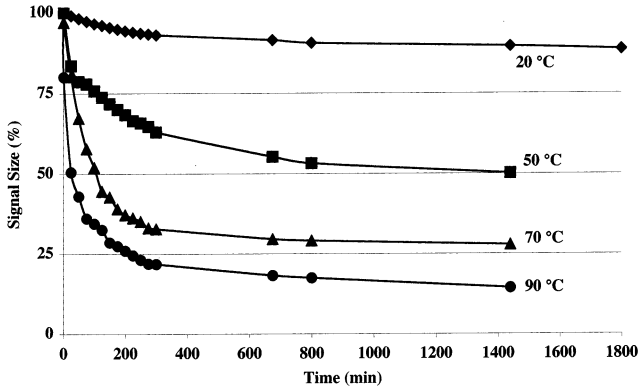

Figure 2. Time-dependent ^{1}H NMR kinetic curves. The curves show the changes of the size of the integrals of the ^{1}H NMR signals (aromatic signals and $-CH_2-$ signal) of complex **7** at a given time at room temperature, 50 °C (squares), 70 °C (triangles), and 90 °C (circles). The integrals of the four signals have been recorded with respect to DMSO as internal standard. The size of the peaks before the addition of TBHP was regarded as 100% value. The relative size of all four signals has been added and divided by four. The relative integral size differences of the four examined signals at a given time are usually less than 5%.

occurred. It was assumed that at 90 °C, a partial thermal decomposition of the Mo(VI)-dioxo catalysts reduces the amount of active species present in the reaction mixtures.[19] The high thermal stability of W(VI)-dioxo complexes is also evident from the fact that the W(VI) compounds can be used for additional catalytic runs, with a new charge of substrate and TBHP, leading again to100% yields within the experimental error range.

Mechanistic Studies: (a) Catalyst Formation. Following the lines of our preceding work on the $Mo(O)_2(X)_2L_2$ system,[28] we assumed that the first step of the catalytic reaction is the formation of the catalyst originating from the reaction of the starting complex $W(O)_2(X)_2L_2$ with TBHP. To check this assumption, we selected complex **7** to study this interaction by ^{1}H NMR spectroscopy. This complex was chosen on the basis of its high solubility and the fact that the CH_3-CH_2- ligand provides a useful probe for detecting spectral changes in addition to the aromatic proton signals. Such a tungsten bound alkyl probe is absent in the $W(O)_2(X)_2L_2$ halide analogues.

Accordingly, complex **7** was reacted at 90, 70, 50, and 20 °C, respectively, with an excess of TBHP in d_6-DMSO and the changes of the spectra were monitored by recording ^{1}H NMR spectra every 25 min for several hours. The results, for a 6-fold excess of TBHP, are summarized in Figure 2 and Table 5. While both the aromatic and aliphatic signals of complex **7** get less pronounced, although always present, a new signal set appears. This new signal set is assigned to a new species **7a**. We assume compound **7a** to be the active species, since the catalyst activity increased with increasing its concentration in the solution and the ^{1}H NMR data fit the expectations about the composition of such an active species. All the aromatic signals in **7** are shifted to higher field (shielded) in **7a**. The CH_3 signal is also slightly more shielded in **7a** than in **7**. In contrast, the W-C*H*$_2$CH$_3$ resonance is more deshielded on going from **7** to **7a**. The new *t*-Bu resonance is observed at a slightly higher field than that of TBHP and is assigned to a W−OO(*t*-Bu)-ligand. These ^{1}H NMR data, in particular the chemical shift variations observed, strongly resemble those observed for the homologous Mo(VI) complexes that we recently examined.[28] In particular, the ^{1}H NMR of $Mo(O)_2(Cl)_2$(4,4′-bis(*n*-hexyl)2,2′-bipyridine) in the presence of excess TBHP also reveals the formation of a new species with similar high-field shifts for all the aromatic protons. Furthermore, the reexamination of the ^{1}H NMR spectrum of $Mo(O)_2(Me)_2$-(4,4′-bis(*n*-hexyl)2,2′-bipyridine), yet unpublished, in the presence of excess TBHP also shows the usual shielding of the aromatic resonances and a deshielding of the Mo-C*H*$_3$ resonance for the new rising species. Unfortunately, the final position and particularly the integral size of the Mo-C*H*$_3$ resonance cannot be detected in the latter case very clearly due to overlap with other aliphatic ligand signals.

As a result of our detailed studies on the nature of the species arising from the reaction of $Mo(O)_2(Cl)_2$(4,4′-bis(*n*-hexyl)2,2′-bipyridine) with TBHP, it was concluded that the Mo atom is surrounded by seven ligands, the chelating ligand L_2, the two ligands X, an oxo and a hydroxy ligand, and the −OO(t-Bu) moiety. IR/Raman examinations of $Mo(O)_2(Cl)_2$-(4,4′-bis(*n*-hexyl)2,2′-bipyridine)/TBHP indicate that the alkylperoxo ligand coordinates in an η^1-manner to the metal center and that the Mo−N interactions are slightly weakened during this process but not broken.[28] The TBHP-hydrogen atom is transferred to one of the terminal oxygen atoms of the metal complex. It is known that hydrogen transfer to the terminal oxygen groups of $M(O)_2(R)_2L_2$ (M = Mo, W) occurs quite readily, depending on the Lewis basicity of the oxo ligands and the acidity of the proton.[1b,14h] The spectroscopic data obtained in the Mo case are also in good accord with theoretical calculations.[28] The ^{1}H NMR spectrum, given in Table 5 for compound **7a**, can be interpreted similar to the case of $Mo(O)_2(Cl)_2$(4,4′-bis(*n*-hexyl)2,2′-bipyridine). The symmetry of the signals, as well as their slight broadening in comparison to complex **7**, is probably due to the fluxionality of the −OH proton and the −OOR group at elevated temperatures.[28] The weakening of the M−N interactions may be responsible for the high-field shift of the ring protons in **7a**, when compared to precursor **7**. This M−N bond weakening may also lead to a stronger electron withdrawing effect on the metal-coordinated R groups to compensate for the weaker influence of L. Therefore, the W-CH_2 protons are low-field shifted in compound **7a**, compared to compound **7**, just as in the case of the Mo−CH_3 signals of the $Mo(O)_2(CH_3)_2$(4,4′-bis(*n*-hexyl)2,2′-bipyridine)/TBHP derivative. Theoretical calculations for the W(VI) case are under way to obtain a better understanding of the details of the differences in the ^{1}H NMR spectra of compounds **7** and **7a**.

It is important to note that the transformation of compound **7** to the new species **7a** is not instantaneous. Moreover, under all examined conditions it takes several hours before reaching an equilibrium between compound **7a** and the precursor complex **7**. If the temperature is lowered after the equilibrium is reached, starting material is reformed and the amount of **7a** is lowered. This shows clearly that **7a** is not the product

Table 4. Rate Constants for the Reactions Depicted in Scheme 1[a]

catalyst	k_1 [$M^{-1}\,s^{-1}$]	k_2 [s^{-1}]	$K_1 = k_1/k_2$	k_3 [$M^{-1}\,s^{-1}$]	k_4 [$M^{-1}\,s^{-1}$]	k_5 [s^{-1}]	k_6 [$M^{-1}\,s^{-1}$]	k_7 [$M^{-1}\,s^{-1}$]
3	0.25[b]	0.021[b]	12[b]	0.6[b]	1.6[b]	0.01[b]	0.006[b]	0.01[b]
	(0.20)[b]	(0.018)[b]	(11)[b]		(1.5)[b]			
	0.0016[c]	0.001[c]	1.6[c]					
7	0.11[b]	0.011[b]	10[b]	0.3[b]	1.4[b]	0.05[b]	0.008[b]	0.01[b]
	(0.13)[b]	(0.01)[b]	(12)[b]					
			1.4[c]					

[a] Values in parentheses were determined by UV/vis experiments from the reaction of TBHP (k_1, k_2) and *t*-BuOH (k_4), respectively, with the complexes **3** and **7** in the absence of substrate. [b] At 85 °C. [c] At 25 °C.

Table 5. ^{1}H NMR Shifts for $W_2(O)_2(Et)_2(L)$ (**7**) and for Its Reaction Product (**7a**) with TBHP at 90 °C in Dimethyl-d_6 Sulfoxide (DMSO)[a]

compound **7**			compound **7a**		
chemical shift [ppm]	signal multiplicity	coupling onstant [Hz]	chemical shift [ppm]	signal multiplicity	coupling constant [Hz]
9.27	d	6	8.57	d	5
8.80	d	1	8.38	d	1
7.79	dd	6; 1	7.45	dd	5; 1
1.45	s		1.35	s	
1.32	t	8	1.27	t	7
0.69	q	8	1.07	q	7
TBHP			W-OOR		
3.22	s, vb		3.36	s, b	
1.14	s		1.12	s	

[a] b = broad. vb = very broad.

of an irreversible reaction and that it is very difficult if not impossible to isolate compound **7a**.

This equilibrium was further characterized by studying the variation of the rate constants and equilibrium constants with temperature in the temperature range from 20 to 90 °C, using NMR and additionally UV/vis spectroscopic methods. Compounds **3** and **7** have been used for the UV/vis experiments. In the case of these two complexes only the ligand X/R is changed, ligand L being the same. Under the conditions described in the Experimental Section, with TBHP present in large excess over the catalyst precursor, the reaction of compounds **3** and **7** respectively with TBHP followed first-order kinetics. The pseudo-first-order rate constants were determined by fitting the absorbance time curves to an exponential decay formula, given as eq 2.

$$\mathrm{Abs}_t = \mathrm{Abs}_0 - (\mathrm{Abs}_0 - \mathrm{Abs}_\infty)\exp(-k_\psi t) \qquad (2)$$

In this equation, Abs_t, Abs_0, and Abs_∞ are the absorbance at any time during the reaction and at the beginning and the end of the reaction, respectively, and k_ψ is the pseudo-first-order rate constant. The second-order rate constants for the reaction of TBHP with the catalyst, k_1, were calculated from eq 3. The resulting rate constants are summarized in Table 4.

$$k_\psi = k_1[\mathrm{TBHP}] \qquad (3)$$

The thermodynamic parameters for the reaction of complex **7** with TBHP were determined from variation of the equilibrium constants with temperature in d_6-DMSO by ^{1}H NMR experiments in the range 20−90 °C; $\Delta H° = +49.0 \pm 2.5$ kJ/mol and $\Delta S° = 166.1 \pm 7$ J/(mol·K) (see Figure 3a). The values and signs of $\Delta H°$ and $\Delta S°$ indicate that the precursor **7** (W-oxo complex) and the catalyst **7a** (W-peroxide complex) have similar stabilities at room temperature, $K_{eq} = 1$ at ∼25 °C (see Figure 3a). These results also help to explain why we were unable to isolate complex **7a** by cooling the reaction mixture.

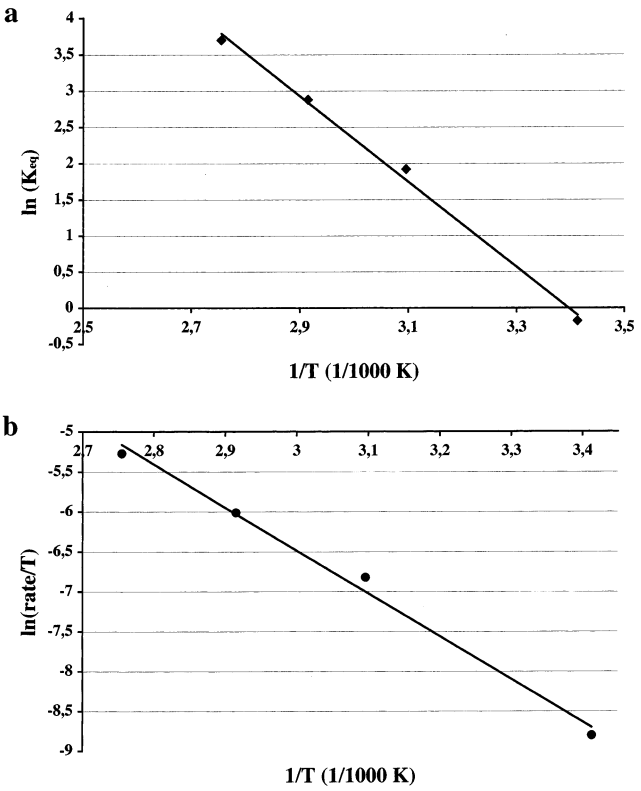

Figure 3. (a) A plot of $\ln(K_{eq})$ against $1/T$ for the reaction of compound **7** with TBHP, based on ^{1}H NMR measurements. The values of $\Delta H° = 49.0 \pm 2.5$ kJ/mol and $\Delta S° = 166 \pm 7$ J/(mol·K) were determined from the slope and the intercept, respectively. (b) A plot of $\ln(\mathrm{rate}/T)$ against $1/T$ for the reaction of compound **7** with TBHP, derived from ^{1}H NMR experiments. The values of $\Delta H^‡ = 44.6 \pm 2.3$ kJ/mol and $\Delta S^‡ = -118 \pm 8$ J/(mol·K) were derived from this graphic.

The activation parameters for the reaction of compound **7** with TBHP in d_6-DMSO were determined from the variation of the second-order rate constant with temperature (20−90 °C), derived from ^{1}H NMR experiments. The values are as follows: $\Delta H^‡ = 44.6 \pm 2.3$ kJ/mol and $\Delta S^‡ = -118 \pm 8$ J/(mol·K) (see Figure 3b). In general, the UV/vis experiments lead to very similar results as the ^{1}H NMR examinations with respect to the velocity of the formation of a new species after the addition of TBHP to the dissolved catalyst precursor.

The rate constants for the reaction of TBHP with the W catalysts are much more sensitive to the temperature than the equilibrium constants ($K_{90}/K_{25} \sim 8$, $k_{90}/k_{25} > 130$, see Table 4). Theoretical calculations are currently under way

to be compared with the values derived from the measurements presented here.

(b) Epoxidation Reaction and Catalyst Blocking. The activation parameters for the epoxidation of cyclooctene with compound **3** and TBHP in CH_3CN were determined from the variation of the second-order rate constant with temperature, derived from GC experiments. The values are the following: $\Delta H^{\ddagger} = 83.4 \pm 4.2$ kJ/mol and $\Delta S^{\ddagger} = -51 \pm 5$ J/(mol·K). The relatively high enthalpy of activation indicates that the rate-controlling step involves more (or stronger) bond breaking than bond formation. This reflects the low activity of the W catalysts at low temperature (<55 °C) and the significant increase in activity with increasing temperature. For the analogous Mo compounds, $\Delta H^{\ddagger}$ is about 20−30 kJ lower. Indeed, Mo(VI) complexes are much more reactive at lower temperatures than the W congeners, as has been stated above. Formation of peroxo-Re species from the reaction of the related Re(VII) complex CH_3ReO_3 (MTO) with H_2O_2 has an activation enthalpy of $\Delta H^{\ddagger} = 29$ kJ/mol,[28] much smaller than the values for both the $Mo(O)_2(X)_2L_2$ and $W(O)_2(X)_2L_2$ complexes. At room temperature, or even below, CH_3ReO_3 shows very high activity toward oxidations with H_2O_2.[29,30] Since MTO does not activate TBHP any comparison of these systems has to be regarded, however, with great caution.

The small negative value of $\Delta S^{\ddagger}$ does not provide useful information about the reaction kinetics, since $\Delta S^{\ddagger}$ depends on the general behavior of the solution (solute−solvent interactions) during the activation step. In the gas phase, without any solvent present, a much higher negative value would be expected for $\Delta S^{\ddagger}$.

A further analysis of the reaction mechanism of the epoxidation reaction can be obtained by means of kinetic simulations with the KINSIM program. The conversion of cyclooctene to cyclooctene oxide GC curves by the $W(O)_2(X)_2L_2$/TBHP catalytic system revealed that the catalytic reaction proceeds rapidly at the beginning of the reaction (5−10% within 5−20 min), then slows down and proceeds almost linearly to nearly 100% conversion within 24 h or more, Figure 4. The catalyst activity is never inhibited completely and, after sufficient time, the epoxidation reaction goes to completeness. This general behavior suggests that during the reaction the catalyst is converted to an inactive species and this species is present in equilibrium with the active catalyst (see Scheme 1). Adding *t*-BuOH to the catalytic reaction mixture slows down the catalytic activity (GC/MS evidence), but does not inhibit the reaction completely. We therefore conclude that *t*-BuOH, formed as byproduct during the olefin epoxidation reaction, acts as competitor with TBHP for the active site of the catalyst. According to UV/vis experiments we performed on the behavior of **3** and **7** in the presence of a 6-fold excess of *t*-BuOH in CH_3CN, *t*-BuOH coordinates more readily to complex **3** than to complex **7**. This slows down the catalytic reaction in the case of compound **3** as catalyst precursor more significantly than in the case of the originally somewhat less active catalyst derived from compound **7** (compare also Table 3).

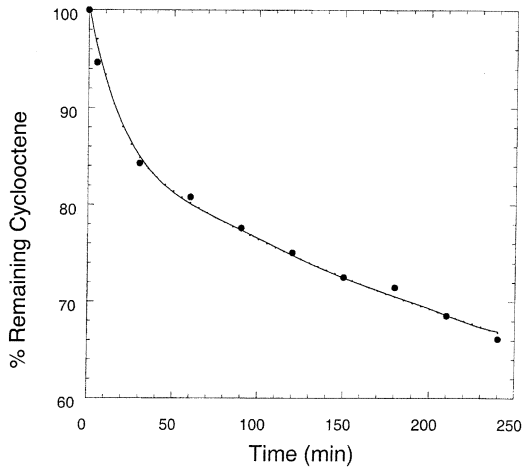

Figure 4. Kinetic profile for the epoxidation of cyclooctene (0.75 M) with TBHP (1.0 M) as catalyzed by complex **3** (0.04 M) at 90 °C in *n*-decane. The circles are experimental values, whereas the solid line represents the calculated data (by KINSIM) based in Scheme 1 and the rate constants k_1, k_2, k_3, k_4, k_5, k_6, and k_7, Table 4.

Scheme 1

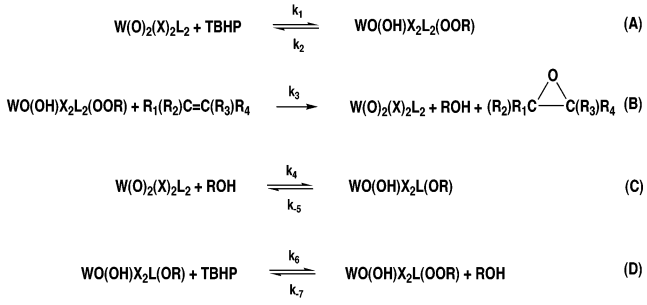

The suggested reaction given in Scheme 1 was confirmed by applying the KINSIM program.[31] The simulated results based on Scheme 1 fit very well with the experimental data (Figure 4). The rate constants k_1 and k_2 (and in case of compound **3** additionally k_4) were determined by UV/vis experiments from the reaction of the catalyst with TBHP (or *t*-BuOH) in the absence of the substrate (cyclooctene). The rate constant k_4 was determined from the reaction of compound **3** with *t*-BuOH. These experimental values of k_1, k_2, and k_4 and the calculated values (evaluated by KINSIM) were in excellent agreement. This confirms the validity of this simulation method in estimating the other rate constants k_3-k_7, based on the suggested mechanism shown in Scheme 1. The values of k_1-k_7, which were evaluated by KINSIM simulation and gave the best fit results to the experimental data, are listed in Table 4. In the case of compounds **3** and **7** the epoxidation of the substrate, cyclooctene, is faster than the formation of the catalyst from the precursor compound. It has to be noted that the reaction of the catalyst precursor with *t*-BuOH does not necessarily have to lead to aprotonation of one of the terminal oxygens attached to the metal center as shown in eq C. *t*-BuOH might be only coordinated as a donor adduct to the metal center. NMR experiments, unfortunately, do not give more insight in this particular case.

(31) Barshop, B. A.; Wrenn, R. F.; Frieden, C. *Anal. Biochem.* **1983**, *130*, 134.

However, as already stated before, spectroscopic and theoretical studies[28] performed on the analogous $Mo(O)_2(X)_2L_2$ system strongly support the reactions presented in eqs A and B (see Scheme 1), namely with respect to the catalyst formation and the O transfer step. Despite the uncertainties in some details, the general picture is quite clear. Only four reactions, A−D, seem to be of influence on the shape of the yield/time curves. Other possible side reactions must therefore play, if any, only a minor role. The rate-determining step in the beginning is the catalyst formation. After some time, when a considerable and still growing amount of alcohol is present in the system, the coordination of the *t*-BuOH slows down the reaction increasingly. It is worth mentioning that the equilibrium constants for the formation of the catalyst from the reactions of **3** and **7** with TBHP are very similar. The difference in reactivity is related, however, to the difference in the rate constants for the formation of the catalytic active species and its reaction with cyclooctene to give cyclooctene epoxide.

(c) Ligand Effects. The influence of the ancilliary ligands X and L in the $W(O)_2(X)_2L_2$ complexes (X = Cl, CH_3, Et; L_2 = DME and diimines) on the epoxide yield can be seen from Table 3. A comparison among the chloro complexes **1**−**5** reveals that compounds **1** and **2** show comparable activity and are more active than the derivatives **3**−**7**, including the alkyl derivatives **6** and **7**. At 90 °C after 6 h, derivative **1** gives an epoxide yield of 91% and complex **2** gives ca. 75%. Steric effects and strong coordination of the Lewis bases might be responsible for the lowering of the activity of compounds **3**−**5** relative to the derivatives **1** and **2**. DME is a much weaker donor than the bidentate nitrogen donor ligands utilized here. The labile coordination of DME makes complex **2** as active as the noncoordinated complex **1**. It has to be assumed that the active species in the case of compound **1** (and probably also **2**) is different from the cases described in the kinetic experiments above. More work to gain insight into the mechanistic behavior of compound **1** is under way.

The strong donor ligands 4,4′-di-*tert*-butyl-2,2′-bipyridine, 2,2-bis(1-pyrazolyl)propane, and *N*,*N*′-dicyclohexane-1,4-diaza-1,3-butadiene significantly lower the activities of complexes **3**−**5**; however, a correlation between their donor ability and the catalyst activity is not clearly evident.

It has to be stated that the activity differences are not due to the solubility of the examined complexes. This is particularly evident by comparing compounds **3**, **6**, and **7**. In that case **6** and **7** are better soluble than complex **3** in all examined solvents but the methyl and ethyl groups lead to a somewhat reduced catalyst activity with respect to the determined TOFs (see Table 3). The same behavior has been observed with the Mo(VI) congeners.[18−22] However, the yield differences are far less pronounced when the yields after longer periods of reaction time are considered. At 90 °C, a yield around 30% is achieved for each of the three complexes after 6 h. Furthermore, after 24 h methyl and ethyl derivatives reach ca. 100% yield while the chloro complex **3** gives only 63% yield. However, after 48 h complex **3** also reaches the 100% yield level. An explanation for this at first glance astonishing behavior has been found in the stronger coordination of *t*-BuOH to compound **3** (see above).

Conclusions

Several complexes of the composition $W(O)_2(Cl)_2L_2$ and $W(O)_2(R)_2L_2$ (R = Me, Et) have been synthesized and examined for their possible application in oxidation catalysis. The examined W(VI) complexes are straightforward to prepare, are stable to air and moisture, and additionally display a quite high thermal stability. Their catalytic activity in olefin epoxidation, represented by their TOF, however, is lower than that of their Mo(VI) congeners and several other well-established transition metal oxo complexes. The reaction temperature also has to be significantly higher than in the case of the Mo(VI) analogues to reach a reasonable reaction time. Nevertheless, the examined W(VI) complexes can be used for several catalytic cycles, seemingly without detectable loss of their catalytic activity. This observation, as well as the high thermal stability of the $W(O)_2(R)_2L_2$-type complexes, leads to the expectation that complexes with chiral groups R* might be good candidates as catalyst precursors in the chiral epoxidation. Work in this direction is currently under way in our laboratories. Due to the relatively sluggish reactions under the applied conditions the tungsten complexes are additionally quite good models for examining the reaction kinetics. As has been assumed in the case of the molybdenum homologues the reaction of $M(O)_2(X)_2L_2$ complexes with TBHP is the rate-determining step and the oxidation byproduct, *t*-BuOH, reacts as a competitor with TBHP. Thus, the activity of the catalyst system decreases during the course of the reaction.

Experimental Section

All preparations and manipulations were carried out under an oxygen- and water-free argon atmosphere with standard Schlenk techniques. $WO(Cl)_4$ and $W(O)_2(Cl)_2$ (**1**) were bought from Aldrich, and $WO(Cl)_4$ was freshly sublimed before using. Solvents were dried by standard procedures, distilled, and kept under argon over molecular sieves. The ligands 4,4′-di-*tert*-butyl-2,2′-bipyridine,[32] 2,2-bis(1-pyrazolyl)propane (BPP),[33] and *N*,*N*′-dicyclohexan-1,4-diaza-1,3-butadiene (CYDAB)[34] and complex $W(O)_2(Cl)_2(DME)$[35] (**2**) were prepared according to the procedures described in the literature. Elemental analyses were performed in the Mikroanalytisches Labor of the TU München, in Garching. ^1H NMR were measured in deuterated solvents (Deutero GmbH, Aldrich) in a Bruker AVANCE DPX 400 spectrometer. IR spectra were recorded on a Perkin-Elmer FTIR spectrometer with KBr pellets as the IR matrix.

Warning: TBHP (in decane) is toxic, possibly mutagen, corrosive and a strong oxidizer. It is a combustible liquid and is readily absorbed through the skin and must be stored below 38 °C (100 °F).

Complexes $W(O)_2(Cl)_2L_2$ (L_2 = 4,4′-di-*tert*-butyl-2,2′-bipyridine, **3**; *N*,*N*′-dicyclohexan-1,4-diaza-1,3-butadiene, **4**; 2,2-bis(1-pyra-

(32) Belser, P.; von Zelewsky, A. *Helv. Chim. Acta* **1980**, *63*, 1675.
(33) Jameson, D.; Castellano, R. *Inorg. Synth.* **1998**, *32*, 51.
(34) Van Koten, G.; Vrieze, K. *Advances in Organometallic Chemistry*; Academic Press: New York, 1982; Vol. 21.
(35) Dreisch, K.; Andersson, C.; Stålhandske, C. *Polyhedron* **1991**, *10*, 2417.

zolyl)-propane, **5**)[35] and WO_2R_2(*t*-bubipy) (R = Me, **6**; Et, **7**)[24] were prepared following modified literature procedures.

Dichlorodioxo(4,4′-di-*tert*-butyl-2,2′-bipyridine)tungsten-(VI) (**3**): $WO(Cl)_4$ (0.17 g, 0.51 mmol) was suspended in 5 mL of CH_2Cl_2, then hexamethyldisiloxane (108 μL, 0. 51 mmol) and 4,4′-di-*tert*-butyl-2,2′-bipyridine (0.15 g, 0.56 mmol) were added subsequently. The resulting dark green solution was stirred at room temperature for 1 h. Addition of 10 mL of diethyl ether led to the formation of a green precipitate, which was washed with diethyl ether and dried in a vacuum. Green crystals of the complex were obtained by diffusion of diethyl ether into a methylene chloride solution of the compound. Yield: 0.19 g (67%). Anal. Calcd for $C_{18}H_{24}Cl_2N_2O_2W$ (555.13): C 38.94, H 4.36, N 5.05. Found: C 38.27, H 3.85, N 4.65. Selective IR (KBr, ν cm^{-1}): 2968, 1613, 1545, 1414, 1250, 1204, 958 (W═O), 917 (W═O), 898, 852. ^{1}H NMR ($CDCl_3$, room temperature, δ ppm): 9.51 (d, 2H), 8.16 (s, 2H), 7.72 (d, 2H), 1.47 (s, 18H).

Dichlorodioxo(*N*,*N*′-dicyclohexan-1,4-diaza-1,3-butadiene)-tungsten(VI) (**4**): $WO(Cl)_4$ (0.17 g, 0.51 mmol) was suspended in 10 mL of CH_2Cl_2, then hexamethyldisiloxane (108 μL, 0. 51 mmol) and CYDAB (0.11 g, 0.51 mmol) were added subsequently. After the mixture was stirred at room temperature for 1 h, the violet precipitate was collected and washed with diethyl ether and dried in a vacuum. Yield: 0.22 g (84%). Anal. Calcd for $C_{14}H_{24}Cl_2N_2O_2W$ (506.74): C 33.15, H 4.74, N 5.53. Found: C 33.02, H 4.72, N 5.42. Selected IR (KBr, ν cm^{-1}): 2942, 2855, 1449, 1402, 1353, 1075, 961, 943 (W═O), 918 (W═O), 883. ^{1}H NMR (DMF-d_7, room temperature, δ ppm): 8.92 (s, 2H), 4.30 (t, 2H), 2.10−1.19 (m, 20H).

Dichlorodioxo(2,2-bis(1-pyrazolyl)propane)tungsten(VI) (**5**): $WO(Cl)_4$ (0.17 g, 0.51 mmol) was suspended in 10 mL of CH_2Cl_2, then hexamethyldisiloxane (108 μL, 0. 51 mmol) and BPP (90 mg, 0.51 mmol) were added subsequently. After the mixture was stirred at room temperature for 1 h, a white precipitate was collected and washed with diethyl ether and dried in a vacuum. Yield: 0.21 g (88%). Anal. Calcd for $C_9H_{12}Cl_2N_4O_2W$ (462.98): C 23.35, H 2.61, N 12.10. Found: C 22.67, H 2.30, N 11.83. Selected IR (KBr, ν cm^{-1}): 3165, 3150, 3137, 1510, 1406, 1237, 1172, 1105, 1083, 1075, 960 (W═O), 920 (W═O), 907, 783, 767, 620.

Dimethyldioxo(4,4′-di-*tert*-butyl-2,2′-bipyridine)tungsten-(VI) (**6**): A solution of $W(O)_2(Cl)_2$(*t*-bubipy) (0.20 g, 0.36 mmol) in 5 mL of THF was cooled to 0 °C, and 0.48 mL (1.44 mmol) of MeMgCl (3.0 M in THF) was added dropwise. The solution was stirred at 0 °C for 0.5 h and then at room temperature for 0.5 h. The solvent was evaporated under vacuum to dryness, and 20 mL of CH_2Cl_2 and 20 mL of H_2O were added to the residue. The CH_2Cl_2 phase was washed with H_2O and dried with $MgSO_4$, filtered, and evaporated to dryness. The yellow product was washed with *n*-hexane and dried under vacuum at room temperature. Yield: 0.11 g (59%). Anal. Calcd for $C_{20}H_{30}N_2O_2W$ (514.18): C 46.71, H 5.88, N 5.45. Found: C 46.52, H 6.60, N 5.11. Selective IR (KBr, ν cm^{-1}): 2961, 2903, 2869, 1613, 1547, 1478, 1410, 1367, 1252, 948 (W═O), 907 (W═O), 889, 869, 849. ^{1}H NMR ($CDCl_3$, room temperature, δ ppm): 9.44 (d, 2H), 8.20 (s, 2H), 7.53 (d, 2H), 1.48 (s, 18H), 0.32 (s, 6H).

Diethyldioxo(4,4′-di-*tert*-butyl-2,2′-bipyridine)tungsten(VI) (**7**): Compound **7** was prepared by the same method with compound **6**. Yield: 38%. Anal. Calcd for $C_{22}H_{34}N_2O_2W$ (542.18): C 48.69, H 6.27, N 5.16. Found: C 47.81, H 6.32, N 4.97. Selective IR (KBr, ν cm^{-1}): 2957, 2866, 1613, 1545, 1479, 1458, 1410, 1365, 1252, 942 (W═O), 897 (W═O), 884, 848. ^{1}H NMR ($CDCl_3$, room temperature, δ ppm): 9.50 (d, 2H), 8.16 (s, 2H), 7.54 (d, 2H), 1.55 (t, 6H), 1.46 (s, 18H), 1.02 (q, 4H).

X-ray crystal structure of complex 3: Crystals of **3** were grown by diffusion of diethyl ether into a methylene chloride solution of the compound. A green crystal measuring 0.56 × 0.25 × 0.15 mm^3 was selected in perfluorinated ether and transferred into a glass capillary that was mounted in a cold N_2 stream on a Nonius KappaCCD device. Preliminary examination and data collection were carried out at the window of a rotating anode X-ray generator (NONIUS FR591, 50 kV, 60 mA, 3.0 kW) with graphite monochromated Mo Kα radiation (λ = 0.71073 Å), controlled by the Collect software package.[36a] Collected images were processed with Denzo.

The unit cell parameters were obtained by full-matrix least-squares refinements of 2089 reflections.[36b] The data collection was performed at 173(1)K (θ-range 1.90° < θ < 25.23°; exposure time 60 s per image; scan width $\Delta\varphi/\Delta\Omega$ = 1°). A total number of 31495 reflections were collected. After merging (R_{int} = 0.042), 3586 reflections remained, which were used for all further calculations. Absorption was corrected during scaling, with μ = 6.057 mm^{-1}. The structure was solved by direct methods and refined with standard difference Fourier techniques.[36c] All hydrogen atoms were placed in calculated positions and included in the structure factor calculations but not refined (riding model). Full-matrix least-squares refinements were carried out by minimizing $\Sigma w(F_o^2 - F_c^2)^2$ with the SHELXL-97 weighting scheme.[36d] The Flack parameter x = 0.024(12) shows that the correct absolute configuration was assumed.

Additional data of the refinement: 232 parameters; 15.5 reflections per parameter; weighting scheme $w = 1/[\sigma^2(F_o^2) + (0.0000P)^2 + 12.6271P]$ where $P = (F_o^2 + 2F_c^2)/3$; shift/error <0.001 in the last cycle of refinement; residual electron density +2.77 eÅ, −1.33 eÅ. Neutral atom scattering factors for all atoms were taken from the *International Tables for X-ray Crystallography*.[36e] All calculations were performed on a PC workstation (Intel Pentium II) with the program PLATON.[36f]

Catalysis reactions with compounds 1−7 as catalysts (GC-experiments): *cis*-Cyclooctene (800 mg, 7.3 mmol), *n*-dibutyl ether (800 mg, internal standard), and 1 mol % (73 μmol) of the compounds **1**−**7** (as catalyst) were added to a thermostated reaction vessel. TBHP (2 mL, 5.5 M in *n*-decane) was added to start the reaction. The course of the reaction was monitored by quantitative GC analysis. Samples were taken and diluted with CH_2Cl_2 and treated with a catalytic amount of MnO_2 and $MgSO_4$ to destroy the peroxide and remove water. The resulting slurry was filtered over a filter equipped Pasteur pipet, and the filtrate was injected into a GC column. The conversion of *cis*-cyclooctene and the yield of cyclooctene epoxide were calculated from a calibration curve (r^2 = 0.999) recorded prior to the reaction course.

UV/vis experiments: All kinetic experiments were carried out under pseudo-first-order conditions with excess TBHP in CH_3CN. The reactions were carried out in quartz cuvettes with a path length

(36) (a) Hooft, R.; Nonius, B. V.;*COLLECT*, Data Collection Software for Nonius Kappa CCD; Delft, The Netherlands, 1998. (b) Otwinowski Z.; Minor W. *Macromolecular Crystallography*, *part A*; Processing of X-ray Diffraction Data Collected in Oscillation Mode, Methods in Enzymology, Vol. 276:Carter, C. W., Sweet, R. M., Jr., Eds.; Academic Press: New York, 1997; pp 307−326. (c) Altomare, A.; Cascarano, G.; Giacovazzo, C.; Guagliardi, A.; Burla, M. C.; Polidori, G.; Camalli, M. *J. Appl. Crystallogr.* **1994**, *27*, 435−441. (d) Sheldrick, G. M. *SHELXL-97*; Universität Göttigen: Göttigen, Germany 1998. (e) *International Tables for Crystallography*; Wilson, A. J. C., Ed.; Kluwer Academic Publishers: Dordrecht, The Netherlands, 1992; Vol. C, Tables 6.1.1.4 (pp 500−502), 4.2.6.8 (pp 219−222), and 4.2.4.2 (pp 193−199). (f) Spek, A. L. *Acta Crystallogr.* **1990**, A46, C34.

of 1 cm (total volume of the cuvettes: 3.0 mL). In a typical experiment, TBHP (0.10 M) was added to a thermostated UV cell (in a water bath) containing a solution of the catalyst **3** (1−2 mM) in 3.0 mL of CH_3CN. The absorbance changes in the region 500−200 nm were recorded with time on a Perkin-Elmer 2λ spectrophotometer. The absorbance time curves were fit to a first-order exponential equation (eq 2) to obtain the values of the pseudo-first-order rate constants, k(obs).

Kinetic NMR experiments: In a typical kinetic ^{1}H NMR experiment 0.023 g (0.045 mmol) of complex **7** was dissolved in 0.5 mL of d_6-DMSO in a NMR tube. The NMR tube was heated to the proper temperature in a Bruker Avance DPX 400 NMR spectrometer. Then an excess of TBHP (e.g. 6- or 1.5-fold) was added and the proceeding of the resulting reaction was recorded each 25 min until no further changes were observed in the spectra. The solvent signal was used as the internal standard for the integration of the NMR signals. After equilibrium was reached the reaction mixture was kept at room temperature for 48 h and then an additional ^{1}H NMR spectrum was measured.

Acknowledgment. W.M.X. acknowledges the Bayerische Forschungsstiftung for a postdoctoral research fellowship, A.M.S. is grateful to the PRAXIS XXI for a postdoctoral research fellowship, S.Z. thanks the Deutsche Forschungsgemeinschaft (DFG), and A.A.A. thanks the Deutscher Akademischer Austauschdienst (DAAD) for a grant. The authors are also grateful to the Fonds der Chemischen Industrie for funding and to Prof. Dr. W. A. Herrmann for continuous support. Jin Zhao is acknowledged for experimental assistance.

Supporting Information Available: An X-ray crystallographic file for compound **3** in CIF format and selected NMR spectra for **7** and a UV/vis spectrum for **3**. This material is available free of charge via the Internet at http://pubs.acs.org.

IC0200085